The electronic spectrum of silicon methylidyne "SiCH..., a molecule with a silicon–carbon triple bond in the excited state

5 AUTHORS, INCLUDING:

Christopher Kingston
National Research Council Canada
45 PUBLICATIONS **791** CITATIONS

The electronic spectrum of silicon methylidyne (SiCH), a molecule with a silicon–carbon triple bond in the excited state

Tony C. Smith, Haiyang Li, and Dennis J. Clouthier[a)]
Department of Chemistry, University of Kentucky, Lexington, Kentucky 40506-0055

Christopher T. Kingston and Anthony J. Merer
Department of Chemistry, University of British Columbia, 2036 Main Mall, Vancouver, British Columbia V6T 1Z1, Canada

The $\tilde{A}\,^2\Sigma^+ - \tilde{X}\,^2\Pi_i$ transition of jet-cooled silicon methylidyne, SiCH, has been recorded by laser-induced fluorescence in the 850–600 nm region. The radical was produced in an electric discharge using tetramethylsilane as the precursor. Fifteen cold bands of SiCH and 16 bands of SiCD have been assigned vibrationally, giving the upper state frequencies as $v'_2 = 715/558\,\text{cm}^{-1}$ and $v'_3 = 1168/1127\,\text{cm}^{-1}$ for SiCH/SiCD. Rotational analysis of the 0^0_0 and 3^3_0 bands for each isotopomer has given the following molecular structures: $r''_0(\text{Si–C}) = 1.692\,52(8)$, $r''_0(\text{C–H}) = 1.0677(4)$, $r'_0(\text{Si–C}) = 1.6118(1)$, and $r'_0(\text{C–H}) = 1.0625(5)$ Å. The silicon–carbon bond length in the $\tilde{X}\,^2\Pi$ ground state of SiCH (electron configuration $\ldots\sigma^2\pi^3$) is typical for a Si=C double bond; in the $\tilde{A}\,^2\Sigma^+$ excited state ($\ldots\sigma^1\pi^4$) it corresponds to a triple bond. This work provides the first experimental measurement of the length of the carbon–silicon triple bond. © *2000 American Institute of Physics.* [S0021-9606(00)00508-0]

I. INTRODUCTION

Experimental and theoretical studies of carbon–silicon multiple bonding have burgeoned since reports of the first physical and chemical characterization of a molecule with a silicon–carbon double bond (1,1,2-trimethylsilaethylene) in 1976.[1,2] A variety of stable compounds containing silicon–carbon double bonds have been synthesized and various transient species such as $H_2C=Si$[3] and $HCSi$[4] have been detected by spectroscopic methods. Despite these successes, it is well-recognized that silicon is very reluctant to form multiple bonds, and compounds containing triply bonded silicon atoms have yet to be detected experimentally. Very recently, we reported the laser spectroscopic detection of the silicon and germanium methylidyne radicals (SiCH and GeCH).[5] In this work, we present a detailed study of silicon methylidyne and show that it has a silicon–carbon triple bond in the first excited electronic state.

Beyond their fundamental significance, small silicon-containing species are also of great importance in astrophysics. After hydrogen and helium, silicon and carbon are among the most abundant elements in the universe and several silicon-based interstellar molecules have been identified, including SiO,[6] SiS,[7] SiC,[8] SiN,[9] SiC_2,[10] SiC_3,[11] SiC_4,[12] and SiH_4.[13] Herbst *et al.*[14] have published model calculations of the gas-phase chemistry of silicon compounds in dense interstellar clouds which suggest that silicon methylidyne (SiCH) and silylidene (H_2CSi) should be relatively abundant, although a recent preliminary search[15] failed to detect H_2CSi. It has also been suggested that carbon–hydrogen–silicon species may be the precursors to the carbon–silicon clusters found in stellar atmospheres,[16] so their detection by radioastronomy would be of great interest.

Organosilicon radicals are also likely to play a role in the chemistry of the chemical vapor deposition of silicon carbide and the formation of hydrogenated amorphous silicon carbide (a-SiCH) films. Such materials are grown from organosilane precursors such as methyltrichlorosilane[17,18] or precursor mixtures of silane and various hydrocarbons[19–21] which are decomposed in hydrogen atmospheres at high temperatures. In the process, a large variety of silicon-based reactive intermediates such as silicon atoms, silicon clusters, silylenes, silylidenes, and organosilicon radicals may be formed and their reactions can influence the composition and electronic properties of the final product. For several years, we have been engaged in spectroscopic studies of such reactive intermediates[22–30] in order to establish sensitive methods for detecting and characterizing them.

The SiCH radical has been detected in neutralization-reionization mass spectrometry studies, proving that it is stable under collision-free conditions.[31] Han *et al.*[32] identified the 1010.4 cm^{-1} Si–C stretching fundamental of SiCH in the photolysis products of silane/methane mixtures in an argon matrix. At about the same time, Cireasa *et al.*[4] reported the near-infrared emission spectrum of SiCH, generated by a direct current discharge through a flowing mixture of hexamethyldisilane and helium. They identified the 3^0_1, 0^0_0, and 3^1_0 bands and obtained rotational constants for the 0^0_0 band. They also suggested that a previous matrix spectrum[33] assigned to SiC should be reassigned as due to SiCH. Unaware of these previous reports, we accidentally discovered the electronic spectrum of jet-cooled SiCH[5] during stimulated emission pumping (SEP) experiments on H_2CSi, produced in a pulsed discharge jet with a tetramethylsilane pre-

cursor. An extensive band system was found in the 850–600 nm region, which was readily assigned as the $\tilde{A}\,^2\Sigma^+ - \tilde{X}\,^2\Pi_i$ electronic transition of linear SiCH. A similar system of bands was found for GeCH,[5] using a tetramethylgermane precursor.

As anticipated by prior ab initio studies,[34,35] the bonding and electronic transitions in SiCH are very different from those in the well-known C_2H radical. C_2H has a $\ldots\pi^4\sigma^1$ configuration and a $^2\Sigma^+$ ground state with Lewis structure $H–C\equiv C\bullet$. The lowest electronic transition[36,37] at 3800 cm^{-1} involves promotion of an electron from the π orbital to the σ orbital, giving a $^2\Pi$ excited state. This molecular orbital picture is consistent with the approximately 0.07 Å increase in the carbon–carbon bond length on electronic excitation. In SiCH, the ground-state electron configuration is $\ldots\sigma^2\pi^3(^2\Pi)$ with the $H–\overset{\bullet}{C}\!=\!Si\!:$ Lewis structure, due to the less favorable mixing or hybridization of the valence shell s and p orbitals of silicon relative to carbon,[38] so that the silicon $3s$ orbital remains doubly occupied. The first electronic transition involves excitation of an electron from the σ to the π orbital, giving a $^2\Sigma^+$ excited state with a carbon–silicon triple bond.

II. EXPERIMENT

Silicon methylidyne was produced in a pulsed discharge jet with tetramethylsilane (TMS) as the precursor. The TMS was cooled to $-55\,°C$ and the vapor seeded into a 30 psi flow of argon which was expanded through a pulsed valve (General Valve, series 9, 0.8 mm orifice). A pulsed electrical discharge apparatus,[24,25] consisting of a pair of disk electrodes mounted in a plastic flow channel, was attached to the exit of the valve. At the appropriate time during the gas flow, a high voltage pulse was applied to the electrodes, creating a glow discharge which dissociated the precursor. For most of these experiments, a small [10 long×6 mm inner diameter] reheat tube[39] was attached to the exit of the pulsed discharge jet. It substantially increased the population of the weaker $^2\Pi_{1/2}$ spin component and also suppressed the excited argon glow from the discharge. Laser-induced fluorescence of the discharge products was excited 10 mm beyond the end of the reheat tube by a pulsed laser and the resulting fluorescence was collected by a lens and focused through appropriate long wave pass filters onto the photocathode of a photomultiplier tube (EMI 9816QB). The pulsed fluorescence signals were processed by gated integrators and recorded digitally.

Low-resolution (0.1 cm^{-1}) survey spectra in the 860–590 nm region were acquired at the University of Kentucky (UK) using a Nd:YAG pumped dye laser (Lumonics HD-500) excitation source. The spectra were calibrated using etalon fringes (FSR 0.65 cm^{-1}), along with optogalvanic lines from various argon-and neon-filled hollow cathode lamps, to an estimated accuracy of 0.05 cm^{-1}. Weak laser-induced fluorescence (LIF) features due to C_2 (Phillips bands),[40] SiH_2 ($\tilde{A}–\tilde{X}$ system),[41] and HCCl ($\tilde{A}–\tilde{X}$ system, from the methyltrichlorosilane precursor, *vide infra*)[42] were also identified among the much stronger bands of SiCH and SiCD in these spectra.

Medium-resolution (0.04 cm^{-1}) spectra of the 0_0^0 bands of SiCH and SiCD in the 854–840 nm region were also obtained at UK using an excimer pumped dye laser equipped with an intracavity angle-tuned etalon (Lambda Physik FL3002E). These spectra were quite difficult to record, due to the abrupt decrease in photomultiplier sensitivity at ~950 nm and the lack of suitable long-wave cutoff filters and wavelength calibration standards in this region. Normally, our photomultiplier is terminated with a small resistor (50–5000 ohms) so that we can use fast timing to discriminate against the initial discharge flash and scattered laser light, but in this very long wavelength region the signals were simply too weak under these conditions and were overwhelmed by scattered light signals at higher input impedances. These problems were overcome by adding a simple gated impedance–switching circuit to the detection system. This circuit takes advantage of the long SiCH fluorescence decay (1–3 μs) and short duration of the scattered laser light pulse (20 ns). A 50 ohm resistor and a fast metal–oxide semiconductor field effect transistor (MOSFET) switch, normally connected to ground, were added in parallel to the 1 MΩ input impedance of the gated integrator. This low impedance input allowed the fast discharge and scattered laser light current pulses to dissipate swiftly. About 200 ns after the laser fired, the switch was opened by a 1–2 msec duration TTL pulse applied to a MOSFET driver. This rapidly switched the input impedance from 50 Ω to 1 MΩ, generating a large, slowly decaying LIF signal voltage, free of interferences, at the gated integrator output.

The 0_0^0 band near-infrared spectra were calibrated using Raman shifting and I_2 LIF techniques similar to those previously described.[43] The high intensity, etalon narrowed output of the Lambda. Physik dye laser operated in the 490–520 nm region with Coumarin 503 was Raman shifted in a high pressure hydrogen cell. The first Stokes beam (615–660 nm) was used to excite an I_2 vapor LIF spectrum for wavelength calibration and the second Stokes beam (830–915 nm) was used to excite the silicon methylidyne LIF spectrum. The medium-resolution spectra were calibrated to an estimated accuracy of 0.003 cm^{-1} for unblended lines.

High-resolution (0.01 cm^{-1}) spectra of the strong 3_0^3 bands of SiCH and SiCD were recorded at the University of British Columbia (UBC) using the same discharge apparatus with helium as the carrier gas. The excitation source was a pulse amplified continuous wave (cw) ring dye laser (Coherent 899-21) operated with DCM in the 625–700 nm region. The cw laser beam (200–400 mW, 500 kHz linewidth) was pulse amplified in an excimer pumped DCM dye amplifier (Lambda Physik FL2003) to yield 10 ns pulses of ~70 MHz linewidth and output power of 10–30 mW at 18 Hz. The resolution of the high-resolution spectra was limited to about 350 MHz by power broadening and the residual Doppler width of the unskimmed molecular beam. The spectra were calibrated using optogalvanic spectra of atomic uranium and interpolation between the atomic lines with fringes from a pressure- and temperature-stabilized 750 MHz etalon system.[44] Unblended lines in the LIF spectra could be measured to an estimated relative precision of about 0.0005 cm^{-1}.

TABLE I. The vibrational frequencies of SiCH and SiCD (in cm^{-1}).

| | $\tilde{X}\,^2\Pi$ | | | | $\tilde{A}\,^2\Sigma^+$ | | | |
| | SiCH | | SiCD | | SiCH | | SiCD | |
Vibration	*Ab initio*[a]	Expt.	Calc.[d]	Expt.	*Ab initio*[e]	Expt.[f]	Calc.[d]	Expt.[f]
$\nu_1(\sigma^+)$C–H stretch	3260.2	⋯	2414	⋯	3249.6	⋯	2415	⋯
$\nu_2(\pi)$ bend	469.9	⋯	363	⋯	848.7	715	554	558
$\nu_3(\sigma^+)$Si–C stretch	1011.9	1013[b]/1010.4[c]	979	977.4[c]	1150.9	1168	1125	1127

[a]From the quartic force field calculated from multireference configuration interaction (MRCI) geometries, Ref. 34.
[b]From the emission spectrum, Ref. 4.
[c]From the matrix infrared absorption spectrum, Ref. 32.
[d]*Ab initio* predictions of the SiCD frequencies were not available in the literature. We calculated them from the SiCH frequencies, including *ab initio* values where necessary, and our experimental geometry, using a simple diagonal force field.
[e]Multiconfiguration self-consistent field–configuration interaction (MCSCF-CI) frequencies of Ref. 35.
[f]This work.

Tetramethylsilane [$(CH_3)_4Si$, Aldrich] was used as received. Fully deuterated tetramethylsilane [$(CD_3)_4Si$] was synthesized[45] by the Grignard reaction of CD_3I (Aldrich) with $SiCl_4$ (Aldrich). The identity and purity of the deuterated precursor were checked by gas-phase infrared spectroscopy. We found that TMS-d_{12} was a much more efficient precursor than commercial TMS, which we deduced must be due to the presence of partially chlorinated methylsilanes in our synthesis product. Subsequent tests with various $(CH_3)_nSiCl_{(4-n)}$ compounds showed that methyltrichlorosilane (CH_3SiCl_3, Aldrich) was the best precursor, giving LIF signals 3–4 times stronger than those from TMS.

III. RESULTS AND ANALYSIS

A. Vibrational analysis

From *ab initio* predictions[34,35] and the results of the rotational analysis of the 0_0^0 band emission spectrum by Cireasa *et al.*,[4] the electronic transition is assigned as $^2\Sigma^+ - {}^2\Pi_i$. SiCH has three vibrations conventionally labeled as ν_1, the C–H stretch, ν_2, the doubly degenerate bend, and ν_3, the Si–C stretch. The theoretically predicted and experimentally observed vibrational frequencies are summarized in Table I.

The $\tilde{A}\,^2\Sigma^+ - \tilde{X}\,^2\Pi_i$ transition of SiCH, as observed by LIF, extends from about 850 to 600 nm; the central portion of it is illustrated in Fig. 1. In agreement with the matrix absorption spectrum[33] and the infrared emission spectra,[4] we assign a strong band with a prominent *Q*-branch at 11 801.2 cm^{-1} as the $^2\Sigma^+ - {}^2\Pi_{3/2}$ component of the 0_0^0 band. The weaker $^2\Sigma^+ - {}^2\Pi_{1/2}$ component, which decreased in intensity when the reheat tube was removed, was found 71.3 cm^{-1} to lower frequency. In SiCD, the $^2\Sigma^+ - {}^2\Pi_{3/2}$ component of the 0_0^0 band was found at 11 743.9 cm^{-1}. The redshift of the 0_0^0 band on deuteration is unexpected; usually a blue shift is found since the vibrational frequencies normally decrease on electronic excitation. The next strong band in the spectrum of SiCH with the same general appearance occurs at 12 968.8 cm^{-1}, and is found to be the first member of a moderately long upper state vibrational progression where the frequency is 1168 cm^{-1}. The corresponding frequency in SiCD is 1127

cm^{-1} so that, in agreement with Cireasa *et al.*,[4] we assign the upper state vibration as the silicon–carbon stretching vibration, ν_3'. Associated with each member of this progression, 3_0^n, is a prominent band with somewhat different appearance lying about 700 cm^{-1} to the blue in SiCH (550 cm^{-1} in SiCD). For various reasons these bands are assigned to the vibronically induced progression $2_0^1 3_0^n$. For a start, their polarizations are different, consistent with the fact that the bending vibration is a non-totally symmetric vibration, of species Π. Figure 2 compares the appearances of the $2_0^1 3_0^2$ and 3_0^3 bands of SiCH. The 3_0^3 band (lower panel) is clearly a perpendicular band, where the spin splitting of the $\tilde{A}\,^2\Sigma^+$ upper state is unresolved; since the $\tilde{X}\,^2\Pi_{3/2}$ lower level has negligible Λ doubling, the band apparently has just four branches, but the two central branches are much stronger than the two outer branches because they are unresolved blends containing *Q* branches. In the parallel-polarized $2_0^1 3_0^2$ band (upper panel), the central branches are less prominent, as shown by the reduced intensity of the main head, because the *Q* branches are much weaker. Also, the $^SR_{21}$ branch is seen to have a small doubling. This is not spin splitting in the
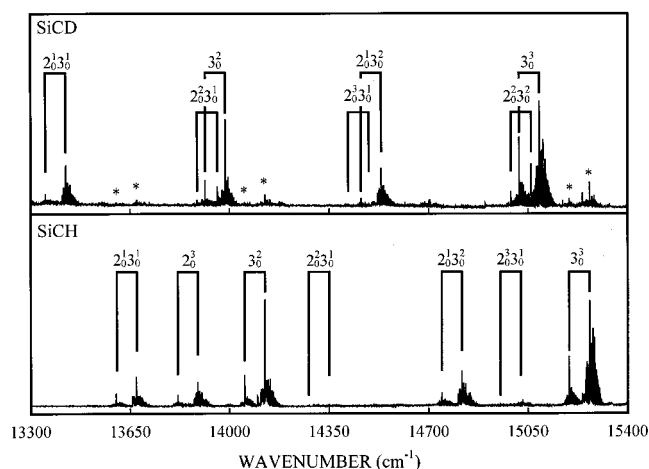

FIG. 1. Portions of the low-resolution LIF spectra of the $\tilde{A}\,^2\Sigma^+ - \tilde{X}\,^2\Pi_i$ band systems of the SiCD and SiCH radicals. An asterisk denotes an impurity band of SiCH in the SiCD spectrum.
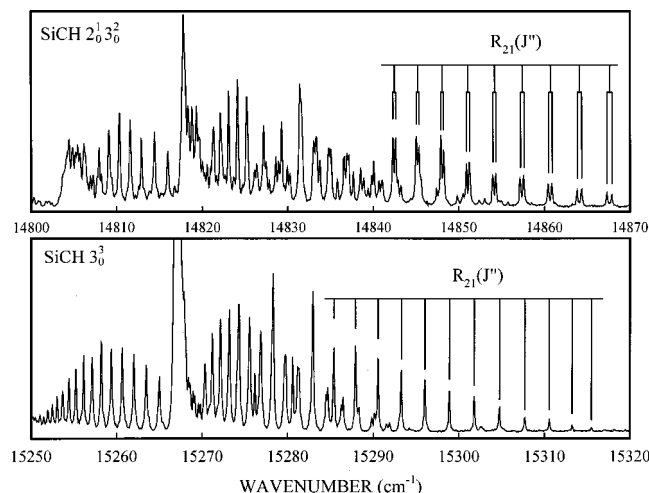
FIG. 2. Medium-resolution spectra of the $^2\Pi_{3/2}$ spin-orbit component of the $2_0^1 3_0^2$ and 3_0^3 bands of SiCH. The R_{21} branch of the $2_0^1 3_0^2$ band exhibits l-type doubling which confirms the Π vibrational symmetry of the upper state.
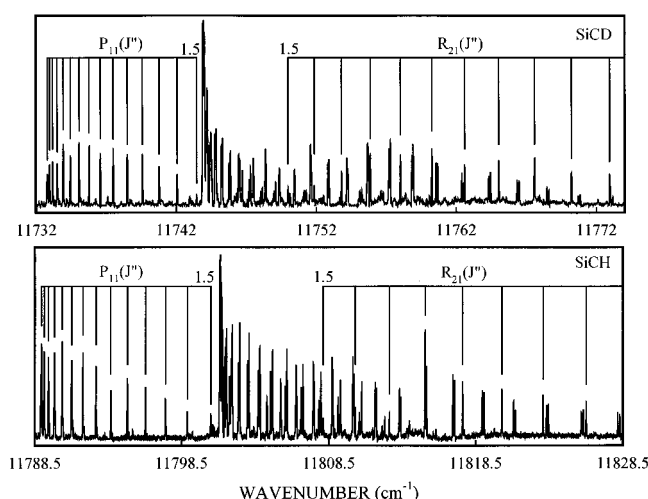

FIG. 3. Medium-resolution spectra of the $^2\Pi_{3/2}$ spin-orbit component of the 0_0^0 bands of SiCH and SiCD, showing the rotational assignments of the P_{11} and R_{21} branches.

$\widetilde{A}\,^2\Sigma^+$ upper state because such splitting does not appear in an $^S R_{21}$ branch, as a result of the rotational selection rules; instead it must be interpreted as the l-type doubling of an upper state vibrational level where the bending vibration is excited. A second argument supporting the assignment to v_2' is the comparatively large isotope ratio of 1.3:1 between SiCH and SiCD, which is only consistent with the bending vibration. Strong vibronic coupling between nearby electronic states, giving rise to intense vibronically induced bands following the selection rule $\Delta v_2 = \pm 1$, is very common in the spectra of linear transition metal-containing compounds;[46–48] it is therefore not surprising that similar coupling occurs in SiCH.

The rest of the spectrum can then be readily assigned as involving combinations of v_2' and v_3', with no evidence of bands involving v_1', the C–H stretching mode. A few weak hot bands were also observed—these will be discussed in a future paper on the Renner–Teller effect in the ground state.[49] The frequency of the central Q-branch maximum of each band and its assignment are presented in Table II and the vibrational frequencies, accurate to about ± 0.5 cm^{-1}, are given in Table I.

B. Rotational analysis

We have rotationally analyzed four bands; the 0_0^0 bands of SiCH and SiCD, recorded at medium resolution at UK, and the 3_0^3 bands of SiCH and SiCD, recorded at high resolution at UBC. The $\widetilde{A}\,^2\Sigma^+ - \widetilde{X}\,^2\Pi_{3/2}$ spin-orbit components of the 0_0^0 bands are shown in Fig. 3; laser-limited linewidths of ~ 0.04 cm^{-1} were achieved, resolving almost all of the rotational structure except the central overlapping Q_{11} and P_{21} branches. A portion of the high-resolution spectrum of the 3_0^3 band of SiCH is presented in Fig. 4, showing the

TABLE II. Q-branch maxima and assignments for the observed vibronic bands of silicon methylidyne (in cm^{-1}).

|	SiCH				SiCD		
Assign.	$^2\Pi_{3/2}$	$^2\Pi_{1/2}$	Comment	Assign.	$^2\Pi_{3/2}$	$^2\Pi_{1/2}$	Comment
0_0^0	11 801.2	11 729.9		0_0^0	11 743.9	11 672.5	
2_0^1	12 516.0	12 444.7	$v_2'=715$	2_0^1	12 301.4	12 230.1	$v_2'=558$
3_0^1	12 968.8	12 897.4	$v_3'=1168$	2_0^2	12 841.3	12 770.3	2_0^1+540
2_0^2	13 203.5	13 132.1	2_0^1+688	3_0^1	12 870.7	12 799.4	$v_3'=1127$
$2_0^1 3_0^1$	13 673.8	13 602.6	3_0^1+705	2_0^3	13 378.9	13 307.6	2_0^2+538
2_0^3	13 889.2	13 817.9	2_0^2+686	$2_0^1 3_0^1$	13 423.4	13 352.3	3_0^1+553
3_0^2	14 124.4	14 053.0	3_0^1+1156	$2_0^2 3_0^1$	13 957.7	13 886.4	$2_0^1 3_0^1+534$
$2_0^2 3_0^1$	14 350.7	14 279.1	$2_0^1 3_0^1+677$	3_0^2	13 985.6	13 914.2	3_0^1+1115
$2_0^1 3_0^2$	14 817.8	14 746.2	3_0^2+693	$2_0^3 3_0^1$	14 489.4	14 418.1	$2_0^2 3_0^1+532$
$2_0^3 3_0^1$	15 025.0	14 953.6	$2_0^2 3_0^1+674$	$2_0^1 3_0^2$	14 533.4	14 462.2	3_0^2+548
3_0^3	15 266.9	15 195.4	3_0^2+1143	$2_0^2 3_0^2$	15 061.5	14 990.2	$2_0^1 3_0^2+528$
$2_0^2 3_0^2$	15 482.8	$\cdots$	$2_0^1 3_0^2+665$	3_0^3	15 090.5	15 019.2	3_0^2+1105
$2_0^1 3_0^3$	15 949.1	$\cdots$	3_0^3+682	$2_0^3 3_0^2$	15 586.1	15 515.0	$2_0^2 3_0^2+525$
3_0^4	16 398.6	16 326.9	3_0^3+1132	$2_0^1 3_0^3$	15 632.0	15 560.7	3_0^3+542
$2_0^2 3_0^3$	16 600.2	16 528.5	$2_0^1 3_0^3+651$	$2_0^2 3_0^3$	16 153.1	16 081.6	$2_0^1 3_0^3+521$
				3_0^4	16 184.3	16 112.9	3_0^3+1094
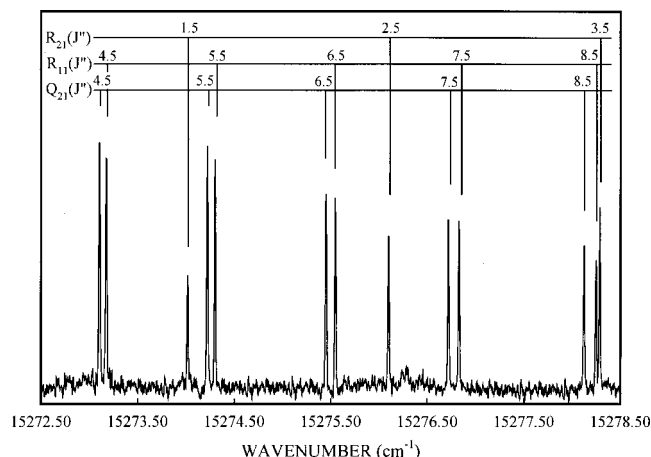
FIG. 4. A portion of the high-resolution spectrum of the 3_0^3 band of SiCH illustrating the upper state spin splittings and the beginning of the R_{21} branch.

beginning of the R_{21} branch and the J-dependent upper state spin-rotation splittings given by the difference between the $Q_{21}(J'')$ and $R_{11}(J'')$ lines. Both sets of spectra were assigned by standard methods using pattern recognition, combination differences, and plots of $R_{11}(J'') - Q_{21}(J'') = \gamma(N + 1/2)$ which confirmed the rotational numbering.

Initial attempts at fitting the 3_0^3 band of SiCH showed that most of the upper levels were substantially perturbed. We therefore elected to use ground-state combination differences from the 0_0^0 and 3_0^3 bands to determine the best possible set of ground-state constants before fitting the upper states. For each band, including both spin components, a data set of strong, symmetric, unblended lines was chosen and all possible combination differences were formed. We refined the ground-state constants by a simultaneous, weighted least-squares fitting of both sets of combination differences, weighting them as the square of the inverse of the estimated precision of the measurements. The high-resolution 3_0^3 band combination differences were given a precision of 0.0007 cm^{-1} and the medium-resolution 0_0^0 band combination differences 0.004 cm^{-1}. A program was written to fit these data to a lower state $^2\Pi$ effective Hamiltonian in the R^2 formulation with the matrix elements given in Table III. The resulting ground-state molecular constants are summarized in Table IV.

A program was written to fit the assigned transitions using the following upper state energy level expressions: for the F_1 levels of e parity,

$$F(N) = T_0 + BN(N+1) - DN^2(N+1)^2 + \tfrac{1}{2}\gamma N$$
$$+ \tfrac{1}{2}\gamma_D N^2(N+1), \tag{1}$$

and for the F_2 levels of f parity,

$$F(N) = T_0 + BN(N+1) - DN^2(N+1)^2 - \tfrac{1}{2}\gamma(N+1)$$
$$- \tfrac{1}{2}\gamma_D N(N+1)^2. \tag{2}$$

In fitting the transitions, the ground-state constants were fixed and the excited state constants were varied as needed; care was taken to eliminate blended, weak, and obviously perturbed transitions from the data set. The resulting constants are given in Table IV and the assignments of the $^2\Pi_{3/2}$ components of the 0_0^0 bands of SiCH and SiCD are summarized in Tables V and VI.

The 0_0^0 bands were free of detectable perturbations but the 3_0^3 bands of both SiCH and SiCD exhibited systematic J-dependent deviations from the calculated energies, as illustrated in Fig. 5. For SiCD, only a single small avoided crossing with a state of lower B value was found in the F_2 component, which approaches the unknown perturbing state from below. In SiCH, the perturbations are substantial and affect both the F_1 and F_2 components in a similar fashion, displacing them to lower energy with increasing J. We found it necessary to constrain the centrifugal distortion constant D to the 0^0 level value since, if varied, it fits the onset of the perturbations by adopting an anomalously large value. The perturbing level must be above 3^3 and have a smaller B value so that the rotational levels of 3^3 catch up at high J. From Table II it is clear that there are no observed transitions very close to 3_0^3, so the perturbing level must either involve v_1' or an overtone of v_2', or it may be a high vibrational level of the ground state. Although the frequency of v_1' is unknown, it must be in the 3000–3250 cm^{-1} range, so that 1^1 falls considerably below 3^3 and $1^1 2^1$ is 250–500 cm^{-1} above 3^3. The course of the v_2' levels is slightly irregular but the level $2^5, l = 1 (\Pi)$ is expected to lie close to the position of the 3^3 level, and could possibly be the cause of the perturbation.

TABLE III. The Hamiltonian matrix for the $^2\Pi$ vibronic states of SiCH in a case (a) basis.

$\lvert ^2\Pi_{1/2}\ e/f\rangle$	$\lvert ^2\Pi_{3/2}\ e/f\rangle$
$B(J+\tfrac{1}{2})^2 - \tfrac{1}{2}A - D[(J+\tfrac{1}{2})^4 + (J+\tfrac{1}{2})^2 - 1]$	$-B[(J+\tfrac{1}{2})^2 - 1]^{1/2} + 2D[(J+\tfrac{1}{2})^2 - 1]^{3/2}$
$-\tfrac{1}{2}A_D(J+\tfrac{1}{2})^2 \mp \tfrac{1}{2}(p+2q)(J+\tfrac{1}{2})$	$\pm \tfrac{1}{2}q(J+\tfrac{1}{2})[(J+\tfrac{1}{2})^2 - 1]^{1/2}$
$\mp \tfrac{1}{2}q_D(J+\tfrac{1}{2})[(J+\tfrac{1}{2})^2 - 1]$	$\pm \tfrac{1}{2}q_D(J+\tfrac{1}{2})[(J+\tfrac{1}{2})^2 - 1]^{3/2}$
$\mp \tfrac{1}{2}(p_D + 2q_D)(J+\tfrac{1}{2})^{3/2}$	$\pm \tfrac{1}{4}(p_D + 2q_D)(J+\tfrac{1}{2})[(J+\tfrac{1}{2})^2 - 1]^{1/2}$
symmetric	$B[(J+\tfrac{1}{2})^2 - 2] - \tfrac{1}{2}A$
	$-D[\{(J+\tfrac{1}{2})^2 - 2\}^2 + (J+\tfrac{1}{2})^2 - 1]$
	$+ \tfrac{1}{2}A_D[(J+\tfrac{1}{2})^2 - 2]$
	$\mp \tfrac{1}{2}q_D(J+\tfrac{1}{2})[(J+\tfrac{1}{2})^2 - 1]$

TABLE IV. Molecular constants (in cm^{-1}) for SiCH and SiCD.[a]

Ground-state constants	SiCH		SiCD	
A	$-69.813\,86_5(19)$	$-69.816(6)$[b]	$-69.942\,39_0(18)$	
B	$0.580\,435_0(13)$	$0.580\,44(9)$	$0.499\,000_3(14)$	
$10^6 D$	$0.544_8(44)$	$0.66(9)$	$0.355_3(42)$	
$10^2 p$	$0.1964_0(50)$	$0.23(3)$	$0.2025_1(42)$	
$10^4 q$	$-0.54_8(13)$	$-1.28(27)$	$-1.16_9(11)$	
root-mean-square (rms) error	$0.000\,68$	0.0058	$0.000\,73$	
Excited state constants	0^0		3^3	0^0	3^3
B	$0.635\,330_4(15)$	$0.635\,39(9)$[b]	$0.621\,713_8(30)$	$0.543\,487_5(24)$	$0.534\,528\,8_6(68)$
$10^6 D$	$0.388_1(36)$	$0.69(12)$	0.4[c]	$0.279_9(54)$	$0.401_5(23)$
$10^2 \gamma$	$0.907_5(11)$	$0.902(18)$	$1.329_1(19)$	$0.744_1(14)$	$0.8467_5(96)$
$10^6 \gamma_D$	$\cdots$	$\cdots$	$\cdots$	$\cdots$	$-1.17_0(46)$
T_0	$11\,766.7363(12)$	$11\,766.7205(27)$	$15\,232.8314(7)$	$11\,709.4734(20)$	$15\,056.3329(4)$
rms error	0.0024	0.0058	$0.000\,78$	0.0024	$0.000\,75$

[a]The number in parentheses are 3σ error limits and are right-justified to the last digit on the line; sufficient additional digits are quoted to reproduce the original data to full accuracy.

[b]From the analysis of the 0_0^0 band emission spectrum, Ref. 4, with the error limits increased to 3σ. A value of $\gamma = 0.000\,26(78)$ was also quoted for the ground state.

[c]Fixed in least-squares analysis; see text.

IV. DISCUSSION

A. Molecular structure

This work reports the first observation of the electronic spectrum of jet-cooled silicon methylidyne. Using the ground and excited state $v = 0$ level rotational constants and assuming the C–H bond length does not change on deuteration, we have calculated the r_0 structures reported in Table VII. The ground-state bond length, $r_0'' = 1.693$ Å, is similar to the *ab initio* predictions,[34,35] and comparable to our experimental value of 1.706 Å for the silicon–carbon double bond length in silylidene (see Table VII). The accepted value for

the length of a standard carbon–silicon double bond[50] is 1.69 Å, in excellent accord with the above gas-phase values.

The excited state Si–C bond length of 1.612 Å is remarkably short, indicating a true triple bond. This is the only experimental value for the length of the carbon–silicon triple bond currently available. It compares favorably with the *ab initio* prediction of 1.604 Å for the bond length of linear silaacetylene, H–C≡Si–H.[51] The silicon methylidyne triple bond is formed by promotion of an electron from a nonbonding σ orbital ($\ldots\sigma^2\pi^3$) to the π orbitals, giving a $\ldots\sigma^1\pi^4$ configuration. The C–H bond length decreases ~ 0.005 Å on

TABLE V. Rotational line frequencies (cm^{-1}) and assignments for the $^2\Sigma^+ - ^2\Pi_{3/2}$ component of the 0_0^0 band of HCSi.

J''	R_{21}	R_{11}	Q_{21}	Q_{11}	P_{21}	P_{11}
1.5	$11\,808.1008(-16)$[a]	$*11\,804.3107(-70)$	$11\,804.2961(11)$			$11\,800.4933(-33)$
2.5	$11\,810.3025(6)$	$*11\,805.2425(-132)$	$11\,805.2231(-8)$			$11\,798.8977(43)$
3.5	$11\,812.6243(36)$	$11\,806.3112(-18)$	$*11\,806.2771(49)$			$11\,797.4137(42)$
4.5	$11\,815.0609(23)$	$11\,807.4877(-19)$	$11\,807.4440(43)$			$11\,796.0454(6)$
5.5	$11\,817.6167(10)$	$11\,808.7872(19)$	$11\,808.7239(-25)$			$11\,794.7991(-4)$
6.5	$11\,820.2902(-17)$	$11\,810.2050(47)$	$11\,810.1368(46)$			$11\,793.6740(5)$
7.5	$11\,823.0823(-48)$	$11\,811.7361(17)$	$11\,811.6585(12)$	$11\,801.5630(-19)$	$11\,801.5001(33)$	$11\,792.6702(34)$
8.5	$*11\,826.0091(78)$	$11\,813.3912(35)$	$11\,813.3039(24)$	$11\,801.9455(-22)$	$11\,801.8729(24)$	$11\,791.7827(34)$
9.5	$11\,829.0379(34)$	$11\,815.1580(-21)$	$11\,815.0609(-39)$	$11\,802.4492(-3)$	$11\,802.3620(-13)$	$11\,791.0116(4)$
10.5	$11\,832.1880(14)$	$11\,817.0518(3)$	$*11\,816.9544(72)$	$11\,803.0694(-11)$	$11\,802.9724(-28)$	$11\,790.3667(45)$
11.5	$11\,835.4573(-2)$	$11\,819.0617(-3)$	$11\,818.9510(24)$	$11\,803.8111(6)$	$11\,803.7044(-17)$	$*11\,789.8381(56)$
12.5	$11\,838.8465(-7)$	$*11\,821.2008(94)$	$*11\,821.0742(53)$	$11\,804.6698(3)$	$11\,804.5533(-28)$	$11\,789.4259(40)$
13.5	$11\,842.3523(-34)$	$11\,823.4366(-32)$	$11\,823.3104(22)$	$11\,805.6456(-20)$	$11\,805.5242(-9)$	$*11\,789.1446(140)$
14.5		$11\,825.8101(30)$	$11\,825.6693(29)$	$11\,806.7437(-8)$	$11\,806.6125(-5)$	
15.5		$11\,828.2953(21)$	$11\,828.1448(14)$	$*11\,807.9499(-105)$	$11\,807.8186(-11)$	
16.5		$11\,830.9018(38)$	$11\,830.7416(24)$	$*11\,809.2888(-63)$	$*11\,809.1378(-76)$	
17.5		$11\,833.6170(-46)$	$*11\,833.4452(-86)$	$*11\,810.7411(-75)$	$*11\,810.5805(-93)$	
18.5		$*11\,836.4576(-63)$	$*11\,836.2779(-91)$	$11\,812.3186(-22)$	$11\,812.1487(-42)$	
19.5		$*11\,839.4098(-150)$	$*11\,839.2301(-87)$	$*11\,814.0028(-90)$	$*11\,813.8232(-116)$	
20.5		$*11\,842.4883(-160)$	$11\,842.3135(43)$	$*11\,815.8003(-211)$	$11\,815.6348(-6)$	
21.5				$*11\,817.7239(-257)$	$*11\,817.5778(233)$	
22.5				$*11\,819.7789(-175)$	$11\,819.5938(16)$	

[a]The numbers in parentheses are observed minus calculated values in units of 10^{-4} cm^{-1}. An asterisk denotes a blended or otherwise poor line not used in the least-squares fit.

TABLE VI. Rotational line frequencies (cm^{-1}) and assignments for the $^2\Sigma^+-{}^2\Pi_{3/2}$ component of the 0_0^0 band of DCSi.

J''	R_{21}	R_{11}	Q_{21}	Q_{11}	P_{21}	P_{11}
1.5	*11 749.9583(−58)[a]	*11 746.7130(−125)	*11 746.6984(−85)			11 743.4568(−3)
2.5	11 751.8316(9)	11 747.5114(−13)	11 747.4872(6)			*11 742.0640(−64)
3.5	11 753.7922(−11)	11 748.3921(−38)	*11 748.3568(−56)			11 740.7776(−21)
4.5	11 755.8538(21)	11 749.3760(10)	11 749.3323(−18)			11 739.5863(13)
5.5	11 758.0071(10)	11 750.4533(32)	11 750.4000(−18)			11 738.4879(16)
6.5	11 760.2525(−38)	11 751.6181(−31)	11 751.5647(−7)			11 737.4863(26)
7.5	11 762.6041(18)	11 752.8895(13)	*11 752.8119(−131)			11 736.5750(−21)
8.5	11 765.0377(−65)	11 754.2532(20)	*11 754.1756(−49)	11 744.4677(35)	11 744.3999(−11)	*11 735.7573(−92)
9.5	11 767.5809(−8)	11 755.7083(−17)	11 755.6307(−12)	*11 744.8451(91)	11 744.7629(−24)	*11 735.0461(−59)
10.5	11 770.2155(5)	*11 757.2699(52)	11 757.1826(34)	11 745.3048(13)	11 745.2274(20)	11 734.4317(−17)
11.5	11 772.9441(2)	11 758.9140(−14)	11 758.8267(44)	11 745.8661(−8)	*11 745.7742(−72)	11 733.9140(31)
12.5	*11 775.7746(61)	*11 760.6695(77)	*11 760.5531(−82)	*11 746.5194(−67)	11 746.4371(40)	11 733.4834(−10)
13.5	11 778.6926(40)	11 762.5021(−19)	*11 762.3904(−57)	*11 747.2888(77)	11 747.1775(−31)	11 733.1495(−43)
14.5	11 781.7027(−16)	11 764.4402(−18)	*11 764.3187(−80)	11 748.1356(38)	11 748.0243(4)	
15.5	11 784.8161(6)	11 766.4776(18)	11 766.3512(−18)	*11 749.0848(66)	11 748.9635(7)	
16.5	11 788.0230(12)	11 768.6017(−36)	*11 768.4704(−47)	11 750.1185(−18)	*11 749.9729(−246)	
17.5		*11 770.8370(65)	11 770.6913(−15)	*11 751.2638(58)	*11 751.1182(−95)	
18.5		11 773.1480(−33)	11 773.0042(−38)	11 752.4916(3)	*11 752.3363(−173)	
19.5		11 775.5707(30)	11 775.4105(−47)	*11 753.7922(−280)	11 753.6709(−42)	
20.5			*11 777.9109(−88)	11 755.2476(31)	11 755.0924(4)	
				11 756.7655(11)	11 756.6055(10)	

[a]The numbers in parentheses are observed minus calculated values in units of 10^{-4} cm^{-1}. An asterisk denotes a blended or otherwise poor line not used in the least-squares fit.

electronic excitation; *ab initio* theory predicts either little change[34] or a slight decrease.[35]

B. Rotational and vibrational analysis

The 0_0^0 band parameters obtained from the rotational analysis of the emission spectrum[4] are in general agreement with the more precise values reported here (Table IV), although the ground-state Λ doubling parameters differ substantially. The $^2\Pi$ state spin-orbit coupling constant [$-69.813\,86(19)$ cm^{-1}] is substantially larger than the *ab initio* prediction[34] of -41.0 cm^{-1}. It has the same sign and approximate magnitude as that of the $\tilde{A}\,^2\Pi_i$ state of the valence isoelectronic molecule SiN (-89.1 cm^{-1}),[52] which happens to be the average (89.0 cm^{-1}) of the atomic spin-
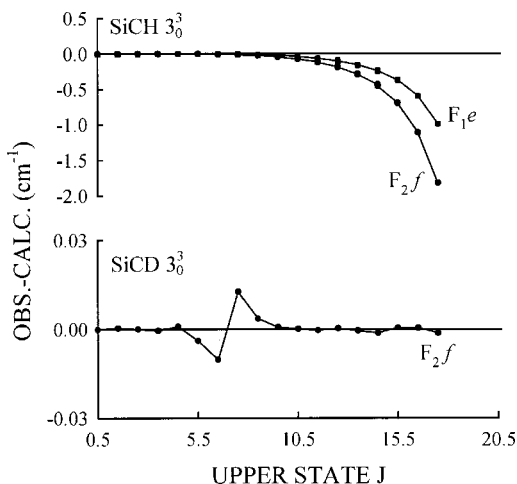

FIG. 5. Observed shifts in the upper state rotational energy levels found in the 3_0^3 bands of SiCH and SiCD. The shifts are plotted as a function of J rather than N to avoid overlap of the F_1 and F_2 curves in the SiCH plot.

orbit constants of silicon (148.9 cm^{-1}) and carbon (29.0 cm^{-1}).[53] One would anticipate that the predominant contribution to the spin-rotation parameter γ in the excited state would come from the interaction with the $^2\Pi_i$ ground state, which in the "pure precession" approximation is given by

$$\gamma = 2ABl(l+1)/(E_\Pi - E_\Sigma), \qquad (3)$$

where A is the spin-orbit coupling constant of the $^2\Pi$ state and l is the angular momentum quantum number of the electron that gives rise to the Σ and Π states. Although this relationship gives the correct sign for γ, it predicts a value of 1.5×10^{-2} cm^{-1}, substantially larger than the experimental value of $0.907(11)\times10^{-2}$ cm^{-1}. Equation (3) also implies that the ratio of the γ values for SiCH and SiCD (1.219) should be the same as the ratio of the rotational constants (1.169), but the discrepancy is considerably larger than the errors in the constants. It is evident that the simple "pure precession" model, with its various approximations,[53] does not work very well in this case.

TABLE VII. Comparison of the experimental (r_0) and *ab initio* structures for the ground and excited states of silicon methylidyne and other carbon–silicon species.

Molecule and state	Source and reference	r (Si–C) Å	r (C–H) Å
SiCH $\tilde{X}\,^2\Pi_i$	Expt'l r_0—this work	1.692 52(8)[a]	1.0677(4)
SiCH $\tilde{X}\,^2\Pi_i$	*ab initio*, Refs. 34/35	1.702/1.710	1.078/1.091
SiC $X\,^3\Pi$	Expt'l r_0, Ref. 56	1.721 87	···
H$_2$C=Si $\tilde{X}\,^1A_1$	Expt'l r_0, Ref. 30	1.706(3)	1.105(3)
SiCH $\tilde{A}\,^2\Sigma^+$	Expt'l r_0—this work	1.6118(1)	1.0625(5)
SiCH $\tilde{A}\,^2\Sigma^+$	*ab initio*, Ref. 34/35	1.587/1.624	1.08/0.084
H–C≡Si–H linear	*ab initio*, Ref. 51	1.604	1.068
HCSiH *trans*-bent	*ab initio*, Ref. 51	1.665	1.077

[a]The numbers in parentheses are three standard errors in units of the last significant figures.

The vibrational analysis can be validated in several ways, although the lack of experimental data for v_1', the C–H stretching frequency, limits the accuracy of the calculations. The vibrational frequencies of SiCD in the excited state can be predicted from the experimentally determined frequencies of SiCH by including the *ab initio* value for v_1'. A simple diagonal force field was determined and the SiCD frequencies calculated from the force constants—the results are given in Table I. The agreement between the observed and calculated frequencies for v_2' and v_3' is excellent. Using the vibrational frequencies in Table I and incorporating experimental data where available, the observed 0_0^0 band shift to lower wave numbers on deuteration is reproduced, although the magnitude of the shift (-57 cm^{-1}) is larger than that calculated (-23 cm^{-1}). Further confirmation of the vibrational numbering comes from the absorption spectrum of SiCH in a neon matrix,[33] originally assigned as due to SiC, but plausibly reassigned by Cireasa *et al.*[4] The spectrum shows a progression of four bands, with the strongest feature at 11 749 cm^{-1}, a harmonic frequency of 1178 cm^{-1}, and an anharmonicity constant of 5 cm^{-1}. Assuming a matrix shift of -52 cm^{-1}, these bands closely match the strong $3_0^n (n=0-3)$ progression in our LIF spectra and the lowest energy feature must be assigned as the 0_0^0 band in each case.

Vibrationally forbidden bands following the selection rule $\Delta v_2 = 1$ are prominent in the $\tilde{A}^2\Sigma^+ - \tilde{X}^2\Pi$ transition of SiCH. Such bands are parallel-polarized ($\Delta K = 0$), although the electronic transition moment is perpendicular. Bands of this type appear as a result of nuclear momentum coupling, which in unsymmetrical linear molecules takes the form of coupling through the bending vibration between electronic states whose Λ values differ by one unit. In this case, the upper $^2\Sigma^+$ state is mixed with a $^2\Pi$ electronic state. Although mixing with higher electronic states is possible, the most likely candidate is the ground state, which is only about 12 000 cm^{-1} distant. The effect of this interaction would be to induce vibrationally forbidden components with $\Delta v_2 = \pm 1$ in the electronic transition between the electronic states, as observed experimentally. For suitably strong mixing, a high density of states, and favorable Franck–Condon factors, we may anticipate that the interaction with higher levels of the ground state would give rise to numerous perturbations in the upper state, as observed in the spectra of WCH[46] and TiCH.[47] From our limited data set, it is evident that such perturbations, if present, are too small to be detected at the present resolution. In this regard, SiCH is probably similar to H$_2$CS[54] and BO$_2$,[55] whose electronic spectra appear unperturbed at Doppler-limited resolution but show numerous tiny level shifts and line doublings at very high resolution.

ACKNOWLEDGMENTS

[1] O. L. Chapman, C.-C. Chang, J. Kolc, M. E. Jung, J. A. Lowe, T. J. Barton, and M. L. Tumey, J. Am. Chem. Soc. **98**, 7846 (1976).

[2] M. R. Chedekel, M. Skoglund, R. L. Kreeger, and H. Shechter, J. Am. Chem. Soc. **98**, 7846 (1976).

[3] H. Leclercq and I. Dubois, J. Mol. Spectrosc. **76**, 39 (1979).

[4] R. Cireasa, D. Cossart, and M. Vervloet, Eur. Phys. J. D **2**, 199 (1998).

[5] T. C. Smith, H. Li, and D. J. Clouthier, J. Am. Chem. Soc. **121**, 6068 (1999).

[6] M. Morris, Astrophys. J. **197**, 603 (1975).

[7] M. Morris, W. Gilmore, P. Palmer, B. E. Turner, and B. Zuckerman, Astrophys. J. **199**, L47 (1975).

[8] J. Cernicharo, C. A. Gottlieb, M. Guelin, P. Thaddeus, and J. M. Vrtilek, Astrophys. J. **341**, L25 (1989).

[9] B. E. Turner, Astrophys. J. **388**, L35 (1992).

[10] P. Thaddeus, S. E. Cummins, and R. A. Linke, Astrophys. J. **283**, L45 (1984).

[11] M. C. McCarthy, A. J. Apponi, and P. Thaddeus, J. Chem. Phys. **110**, 10645 (1999).

[12] M. Ohishi, N. Kaifu, K. Kawaguchi, A. Murakami, S. Saito, S. Yamamoto, S. Ishikawa, Y. Fujita, Y. Shiratori, and W. M. Irvine, Astrophys. J. **345**, L83 (1989).

[13] D. M. Goldhaber and A. L. Betz, Astrophys. J. **279**, L55 (1984).

[14] E. Herbst, T. J. Miller, S. Wlodek, and D. K. Bohme, Astron. Astrophys. **222**, 205 (1989).

[15] M. Izuha, S. Yamamoto, and S. Saito, J. Chem. Phys. **105**, 4923 (1996).

[16] S. Wlodek, A. Fox, and D. K. Bohme, J. Am. Chem. Soc. **113**, 4461 (1991), and references therein.

[17] T. Kaneko, H. Sone, N. Miyakawa, and M. Naka, Jpn. J. Appl. Phys., Part 1 **38**, 2089 (1999).

[18] B-T. Lee, D-K. Kim, C-K. Moon, J. K. Kim, Y. H. Seo, K. S. Nahm, H. J. Lee, K-W. Lee, K-S. Yu, Y. Kim, and S. J. Jang, J. Mater. Res. **14**, 24 (1999).

[19] I. Pereya, M. N. P. Carreno, M. H. Tabacniks, R. J. Prado, and M. C. A. Fantini, J. Appl. Phys. **84**, 2371 (1998).

[20] *Tetrahedrally-Bonded Amorphous Semiconductors*, edited by D. Adler and H. Fritzsche (Plenum, New York, 1985).

[21] T. Stapinski, G. Ambrosone, U. Coscia, F. Giorgis, and C. F. Pirri, Physica B **254**, 99 (1998).

[22] W. W. Harper, J. Karolczak, D. J. Clouthier, and S. C. Ross, J. Chem. Phys. **103**, 883 (1995).

[23] J. Karolczak, R. H. Judge, and D. J. Clouthier, J. Am. Chem. Soc. **117**, 9523 (1995).

[24] H. Harjanto, W. W. Harper, and D. J. Clouthier, J. Chem. Phys. **105**, 10189 (1996).

[25] W. W. Harper, D. A. Hostutler, and D. J. Clouthier, J. Chem. Phys. **106**, 4367 (1997).

[26] W. W. Harper and D. J. Clouthier, J. Chem. Phys. **106**, 9461 (1997).

[27] W. W. Harper, E. A. Ferrall, R. K. Hilliard, S. M. Stogner, R. S. Grev, and D. J. Clouthier, J. Am. Chem. Soc. **119**, 8361 (1997).

[28] W. W. Harper, D. J. Clouthier, and R. H. Judge, J. Mol. Spectrosc. **189**, 46 (1998).

[29] D. J. Clouthier, W. W. Harper, C. M. Klusek, and T. C. Smith, J. Chem. Phys. **109**, 7827 (1998).

[30] W. W. Harper, K. Waddell, and D. J. Clouthier, J. Chem. Phys. **107**, 8829 (1997).

[31] R. Srinivas, D. Sulzle, and H. Schwarz, J. Am. Chem. Soc. **113**, 52 (1991).

[32] D. S. Han, C. M. L. Rittby, and W. R. M. Graham, J. Chem. Phys. **108**, 3504 (1998).

[33] M. Grutter, P. Freivogel, and J. P. Maier, J. Phys. Chem. **101**, 275 (1997).

[34] J. M. Robbe, H. Lavendy, J. P. Flament, and G. Chambaud, Chem. Phys. Lett. **267**, 91 (1997).

[35] H. Lavendy, J. M. Robbe, D. Duflot, and J. P. Flament, AIP Conference Processing **312**, 343 (1994).

[36] R. F. Curl, P. G. Carrick, and A. J. Merer, J. Chem. Phys. **82**, 3479 (1985).

[37] P. G. Carrick, A. J. Merer, and R. F. Curl, J. Chem. Phys. **78**, 3652 (1983).

[38] W. Kutzelnigg, Angew. Chem. Int. Ed. Engl. **23**, 272 (1984).

[39] D. L. Michalopoulos, M. E. Geusic, P. R. R. Langridge-Smith, and R. E. Smalley, J. Chem. Phys. **80**, 3556 (1984).

[40] J. G. Phillips, Astrophys. J. **107**, 389 (1948).

[41] M. Fukushima, S. Mayama, and K. Obi, J. Chem. Phys. **96**, 44 (1992).

[42] A. J. Merer and D. N. Travis, Can. J. Phys. **44**, 525 (1966).

[43] J. Karolczak and D. J. Clouthier, Rev. Sci. Instrum. **61**, 1607 (1990).

[44] A. G. Adam, A. J. Merer, D. M. Steunenberg, M. C. L. Gerry, and I. Ozier, Rev. Sci. Instrum. **60**, 1003 (1989).

[45] J. G. Aston, R. M. Kennedy, and G. H. Messerly, J. Am. Chem. Soc. **63**, 2343 (1941).

[46] M. Barnes, D. A. Gillett, A. J. Merer, and G. F. Metha, J. Chem. Phys. **105**, 6168 (1996).

[47] M. Barnes, A. J. Merer, and G. F. Metha, J. Mol. Spectrosc. **181**, 168 (1997).

[48] A. G. Adam, K. Athanassenas, D. A. Gillett, C. T. Kingston, A. J. Merer, J. R. D. Peers, and S. J. Rixon, J. Mol. Spectrosc. **196**, 45 (1999).

[49] T. C. Smith, H. Li, D. J. Clouthier, and A. J. Merer, to be submitted.

[50] H. S. Gutowsky, J. Chen, P. J. Hajduk, J. D. Keen, C. Chuang, and T. Emilsson, J. Am. Chem. Soc. **113**, 4747 (1991).

[51] R. Stegmann and G. Frenking, J. Comput. Chem. **17**, 781 (1996).

[52] C. Yamada and E. Hirota, J. Chem. Phys. **82**, 2547 (1985).

[53] H. Lefebyre-Brion and R. W. Field, *Perturbations in the Spectra of Diatomic Molecules* (Academic, New York, 1986).

[54] D. J. Clouthier, G. Huang, A. G. Adam, and A. J. Merer, J. Chem. Phys. **101**, 7300 (1994).

[55] A. G. Adam, A. J. Merer, and D. M. Steunenberg, J. Chem. Phys. **92**, 2848 (1990).

[56] C. R. Brazier, L. C. O'Brien, and P. F. Bernath, J. Chem. Phys. **91**, 7384 (1989).